A proxy for atmospheric daytime gaseous sulfuric acid concentration in urban Beijing

Yiqun Lu[1], Chao Yan[2], Yueyun Fu[3], Yan Chen[4], Yiliang Liu[1], Gan Yang[1], Yuwei Wang[1], Federico Bianchi[2], Biwu Chu[2], Ying Zhou[5], Rujing Yin[3], Rima Baalbaki[2], Olga Garmash[2], Chenjuan Deng[3], Weigang Wang[4], Yongchun Liu[5], Tuukka Petäjä[2,5,6], Veli-Matti Kerminen[2], Jingkun Jiang[3], Markku Kulmala[2,5], Lin Wang[1,7,8*]

[1] Shanghai Key Laboratory of Atmospheric Particle Pollution and Prevention (LAP[3]), Department of Environmental Science & Engineering, Jiangwan Campus, Fudan University, Shanghai 200438, China

[2] Institute for Atmospheric and Earth System Research / Physics, Faculty of Science, University of Helsinki, 00014 Helsinki, Finland

[3] State Key Joint Laboratory of Environment Simulation and Pollution Control, School of Environment, Tsinghua University, Beijing 100084, China

[4] Institute of Chemistry, Chinese Academy of Sciences, Beijing 100190, China

[5] Aerosol and Haze Laboratory, Advanced Innovation Center for Soft Matter Science and Engineering, Beijing University of Chemical Technology, Beijing 100029, China

[6] Joint International Research Laboratory of Atmospheric and Earth System Sciences (JirLATEST), School of Atmospheric Sciences, Nanjing University, Nanjing 210023, China

[7] Institute of Atmospheric Sciences, Jiangwan Campus, Fudan University, Shanghai 200438, China

[8] Shanghai Institute of Pollution Control and Ecological Security, Shanghai 200092, China

* *Corresponding Author: L.W., email, lin_wang@fudan.edu.cn; phone, +86-21-31243568.*

Abstract. Gaseous sulfuric acid is known as one of the key precursors for atmospheric new particle formation processes, but its measurement remains a difficulty. A proxy method that is able to derive gaseous sulfuric acid concentrations from parameters that can be measured relatively easily and accurately is therefore highly desirable for the atmospheric chemistry community. Although such methods are available for clean atmospheric environments, a proxy that works well in a polluted atmosphere, such as those in Chinese megacities, is yet to be developed. In this study, the gaseous sulfuric acid concentration was measured in February-March, 2018, in urban Beijing by a nitrate based - Long Time-of-Flight Chemical Ionization Mass Spectrometer (LToF-CIMS). A number of atmospheric parameters were recorded concurrently including the ultraviolet radiation B (UVB) intensity, concentrations of O_3, NO_x (sum of NO and NO_2), SO_2 and HONO, and aerosol particle number size distributions. A proxy for atmospheric daytime gaseous sulfuric acid concentration was derived through a statistical analysis

method by using the UVB intensity, [SO_2], condensation sink (CS), [O_3], and [HONO] (or [NO_x]) as the predictor variables. In this proxy method, we considered the formation of gaseous sulfuric acid from reactions of SO_2 and OH radicals during the daytime, and loss of gaseous sulfuric acid due to its condensation onto the pre-existing particles. In addition, we explored formation of OH radicals from the conventional gas-phase photochemistry using ozone as a proxy and from the photolysis of HONO using HONO (and subsequently NO_x) as a proxy. Our results showed that the UVB intensity and [SO_2] are dominant factors for the production of gaseous sulfuric acid, and that the simplest proxy could be constructed with the UVB intensity and [SO_2] alone. When the OH radical production from both homogenously- and heterogeneously-formed precursors were considered, the relative errors were reduced up to 20 %.

1 Introduction

Gaseous sulfuric acid (H_2SO_4) is a key precursor for atmospheric new particle formation (NPF) processes (Kerminen, 2018; Kirkby et al., 2011; Kuang et al., 2008; Kulmala and Kerminen, 2008; Sipilä et al., 2010). A number of atmospheric nucleation mechanisms including H_2SO_4-H_2O binary nucleation (Benson et al., 2008; Duplissy et al., 2016; Kirkby et al., 2011), H_2SO_4-NH_3-H_2O ternary nucleation (Kirkby et al., 2011; Korhonen et al., 1999; Kürten et al., 2015), and H_2SO_4-DMA-H_2O ternary nucleation (Almeida et al., 2013; Jen et al., 2014; Kürten et al., 2014; Petäjä et al., 2011; Yao et al., 2018) involve the participation of gaseous sulfuric acid molecules. In addition, the condensation of gaseous sulfuric acid onto newly-formed particles contributes to their initial growth (Kuang et al., 2012; Kulmala et al., 2013). Quantitative assessments of the contribution of gaseous sulfuric acid to both the new particle formation rates and the particle growth rates require real-time measurements of gaseous sulfuric acid concentrations prior to and during the NPF events (Nieminen et al., 2010; Paasonen et al., 2010).

Measurements of gaseous sulfuric acid in the lower troposphere are challenging because its ambient concentration is typically quite low (10^6-10^7 molecule cm^{-3}) (Kerminen et al., 2010; Mikkonen et al., 2011). Reported real-time measurements of gaseous sulfuric acid are currently based on Chemical Ionization Mass Spectrometry with NO_3^- and its ligands as reagent ions (nitrate CIMS) because nitrate CIMS with an atmospheric pressure interface (API) has a low detection limit for the atmospheric concentration range of gaseous sulfuric acid (Jokinen et al., 2012), and a constant fraction of sulfuric acid present in the air sample will be ionized by excessive nitrate ions in CIMS under constant instrumental conditions (Kürten et al., 2012; Zheng et al., 2010), which makes the quantification of gaseous sulfuric acid feasible.

Arnold and Fabian (1980) measured the negative ions in the stratosphere and derived the concentration of stratospheric gaseous sulfuric acid from the fractional abundances of a series of stratospheric negative ions as well as the rate constants. Later, real-time measurement of sulfuric acid in the lower troposphere was performed using nitrate CIMS (Eisele and Tanner, 1993), with laboratory calibrations by production of known concentrations of OH radicals that are titrated into gaseous sulfuric acid. Thereafter, measurements of sulfuric acid using CIMS have been performed around the world (e.g., Berresheim et al., 2000; Bianchi et al., 2016; Chen et al., 2012; Jokinen et al., 2012; Kuang et al., 2008; Kürten et al., 2014; Kurtén et al., 2011; Petäjä et al., 2009;

Weber et al., 1997; Zheng et al., 2011), and CIMS has been proven to be a robust tool for gaseous sulfuric acid detection. However, sulfuric acid measurements are still rather sparse because of the high cost of the CIMS instrument and the extensive demand of specialized expertise on the instrument calibration, maintenance, and data processing, etc. Therefore, a proxy for gaseous sulfuric acid concentration is highly desirable.

Proxies for the estimation of atmospheric gaseous sulfuric acid concentrations were previously developed to approximate measurement results of sulfuric acid in Hyytiälä, Southern Finland (Petäjä et al., 2009), assuming that gaseous sulfuric acid is formed from reactions between SO_2 and OH radicals, and lost due to its condensation onto pre-existing particles. The derived simplest proxy can be written as Eq. (1) below, and the authors recognized that the proxies might be site-specific and should be verified prior to utilization in other environments.

$$[\boldsymbol{H_2SO_4}] = \boldsymbol{k} \cdot \frac{[\boldsymbol{SO_2}] \cdot (\boldsymbol{UVB\ \ or\ \ Global\ \ radiation})}{\boldsymbol{CS}} \qquad (\mathbf{1})$$

Mikkonen et al. (2011) later developed a couple of statistical proxies based on measurements of sulfuric acid in six European and North American sites, including urban, rural and forest areas. Their results showed that the radiation intensity and $[SO_2]$ are the most important factors to determine the concentration of sulfuric acid, and that the impact of condensation sink (CS) for gaseous sulfuric acid, is generally negligible. In several proxies developed by Mikkonen et al. (2011), the correlation between the gaseous sulfuric acid concentration and CS is positive, which is against what one would expect because a larger CS normally leads to a faster loss for gaseous sulfuric acid. In addition, the performance of a proxy equation is site-specific because of varying atmospheric conditions from one site to another, which implies that the proxy suggested by Mikkonen et al. (2011) might not work well in locations with atmospheric environments different from those in the six sites of that study.

Beijing is a location with typical values of CS (*e.g.*, 0.01-0.24 s^{-1} in the 5-95% percentiles in this study) being 10-100 times higher (Herrmann et al., 2014; Wu et al., 2007; Xiao et al., 2015; Yue et al., 2009; Zhang et al., 2011) and typical SO_2 concentrations being 1-10 times higher (Wang et al., 2011a; Wu et al., 2017) than those in Europe and North America (Dunn et al., 2004; Mikkonen et al., 2011), yet measured gaseous sulfuric acid concentrations are relatively similar in these environments (Chen

et al., 2012; Smith et al., 2008; Wang et al., 2011b; Zheng et al., 2011). Whether previous proxies developed for European and North American sites work in Beijing remains to be tested. Furthermore, in addition to the gas phase reaction between $O(^1D)$ and water molecules (Crutzen and Zimmermann, 1991; Logan et al., 1981), photolysis of HONO could be a potentially important source of OH radicals in the atmosphere in the early morning (Alicke et al., 2002, 2003; Elshorbany et al., 2009; Li et al., 2012) and during the daytime (Acker et al., 2005; Aumont et al., 2003; Kleffmann, 2007). An experimental study measuring HONO near the surface layer estimated that HONO was a main contributor to OH production in Beijing, with HONO's contribution being larger than 70 % at around 12:00-13:00, except for summer when the contribution of O_3 dominated (Hendrick et al., 2014). Given the distinct characteristics of these two OH radical formation pathways, they both should be included and evaluated separately when a proxy for atmospheric gaseous sulfuric acid concentration is being built. The reactions between SO_2 and Criegee intermediates formed from the ozonolysis of atmospheric alkenes could be a potential source of sulfuric acid only in the absence of solar radiation (Boy et al., 2013; Mauldin et al., 2012), so these reactions are expected to provide a minor contribution to the formation of gaseous sulfuric acid during the daytime in urban Beijing.

In this study, gaseous sulfuric acid concentration was measured by a Long Time-of-Flight Chemical Ionization Mass Spectrometer (LToF-CIMS) in February - March, 2018, in urban Beijing. A number of atmospheric parameters were recorded concurrently, including the ultraviolet radiation B (UVB) intensity, concentrations of O_3, NO_x, SO_2 and HONO, and particle number size distributions. The objective of this study is to develop a robust daytime gaseous sulfuric acid concentration proxy for Beijing, a representative Chinese megacity with urban atmospheric environments.

2 Ambient measurements

An intensive campaign was carried out from 9 February to 14 March, 2018 on the fifth floor of a teaching building in the west campus of Beijing University of Chemical Technology ($39^\circ 94' N, 116^\circ 30' E$). This monitoring site is 2 km to the west of the West 3rd Ring Road and surrounded by commercial properties and residential dwellings. Hence, this station can be regarded as a representative urban site.

The sulfuric acid concentration was measured by a LToF-CIMS (Aerodyne Research, Inc.) equipped with a nitrate chemical ionization source. Ambient air was

drawn into the ionization source through a stainless-steel tube with a length of 1.6 m and a diameter of 3/4 inch. A mixture of a 3 standard cubic centimeter per minute (sccm) ultrahigh purity nitrogen flow containing nitric acid and a 20 standard liter per minute (slpm) pure air flow supplied by a zero-air generator (Aadco 737, USA), together as a sheath flow, was introduced into a PhotoIonizer (Model L9491, Hamamatsu, Japan) to produce nitrate reagent ions. This sheath flow was then introduced into a co-axial laminar flow reactor concentric to the sample flow. Nitrate ions were pushed to the middle of the sample flow under an electric field and subsequently charged sample molecules. For example, the atmospheric H_2SO_4 molecules would be charged by nitrate reagent ion $NO_3^-(HNO_3)_{0\text{-}2}$ and mainly produce HSO_4^- ions (m/z = 96.9601 Th), $HSO_4^-\cdot HNO_3$ ions (m/z = 159.9557 Th), and $HSO_4^-\cdot(HNO_3)_2$ ions (m/z = 222.9514 Th). In addition, $HSO_4^-\cdot H_2SO_4$ ions (m/z = 194.9275 Th) were formed from ion-induced clustering of neutral sulfuric acid and bisulfate ions within the LToF-CIMS ion reaction zone, and also from the evaporation of dimethylamine (DMA) and the replacement of one molecule of H_2SO_4 with one bisulfate ion, HSO_4^-, during the NO_3^- reagent ion charging of a stabilized neutral sulfuric acid dimer in the real atmosphere in presence of DMA or a molecule that works in the same way as DMA. During the campaign, the sample flow rate was kept at 8.8 slpm, since mass flow controllers fixed the sheath flow rate and the excess flow rate, and the flow into the mass spectrometer (around 0.8 slpm) was fixed by the size of a pinhole between the ionization source and the mass spectrometer. The concentration of gaseous sulfuric acid was then determined by Eq. (2).

$$[\boldsymbol{H_2SO_4}] = \frac{\boldsymbol{HSO_4^-}\cdot(\boldsymbol{HNO_3})_{\boldsymbol{0-2}} + \boldsymbol{HSO_4^-}\cdot\boldsymbol{H_2SO_4}}{\boldsymbol{NO_3^-(HNO_3)_{0-2}}}\cdot\boldsymbol{C} \qquad (2)$$

where C is the calibration coefficient, and $NO_3^-(HNO_3)_{0\text{-}2}$, $HSO_4^-\cdot(HNO_3)_{0\text{-}2}$ and $HSO_4^-\cdot H_2SO_4$ represent the signals of corresponding ions and are in units of counts per second (cps). The unit of resulting $[H_2SO_4]$ is molecule cm^{-3}. The CIMS was calibrated during the campaign with a home-made calibration box that can produce adjustable concentrations of gaseous sulfuric acid from SO_2 and OH radicals following the protocols in previous literatures (Kürten et al., 2012; Zheng et al., 2015). We obtain a calibration coefficient of 3.79×10^9 molecule cm^{-3} for our instrument and use 1.1×10^{10} molecule cm^{-3} as the effective calibration coefficient, after taking into account the diffusion losses in the stainless-steel tube and the nitrate chemical ionization source.

The obtained mass spectra were analyzed with a tofTools package based on the MATLAB software (Junninen et al., 2010).

Ambient particle number size distributions down to about 1 nm were measured using a combination of a scanning mobility particle sizer spectrometer (SMPS) equipped with a diethylene glycol-based condensation particle counter (DEG-CPC, ~1-10 nm) and a conventional particle size distribution system (PSD, ~3 nm - 10 μm) consisting of a pair of aerosol mobility spectrometers developed by Tsinghua University (Cai et al., 2017; Jiang et al., 2011; Liu et al., 2016). The values of CS were calculated following Eq. (3) (Dal Maso et al., 2002):

$$CS = 2\pi D \int_0^\infty D_p \beta_m(D_p) n(D_p) dD_p = 2\pi D \sum_i \beta_i D_{pi} N_i \qquad (3)$$

where D_{pi} is the geometric mean diameter of particles in the size bin i and N_i is the particle number concentration in the corresponding size bin. D is the diffusion coefficient of gaseous sulfuric acid, and β_m represents a transition-regime correction factor dependent on the Knudsen number (Fuchs and Sutugin, 1971; Gopalakrishnan and Hogan Jr., 2011).

SO_2, O_3 and NO_x concentrations were measured using a SO_2 analyzer (Model 43i, Thermo, USA), a O_3 analyzer (Model 49i, Thermo, USA) and a NO_x analyzer (Model 42i, Thermo, USA) with the detection limits of 0.1 ppbv, 0.5 ppbv and 0.4 ppbv, respectively. The above instruments were pre-calibrated before the campaign. The UVB (280 - 315 nm) intensity (UV-S-B-T, KIPP&ZONEN, The Netherlands) was measured on the rooftop of the building. Atmospheric HONO concentrations were measured by a home-made HONO analyzer with a detection limit of 0.01 ppbv (Tong et al., 2016).

Particle number size distributions and concentrations of gaseous sulfuric acid, SO_2, O_3, NO_x and HONO were recorded with a time resolution of 5 min, and the UVB intensity with time resolution of 1 min. A linear interpolation method was used for deriving the variables with the same time intervals, *i.e.*, 5 min. Only data between local sunrise and sunset were used in the subsequent analysis.

3 Development of a proxy for atmospheric gaseous sulfuric acid

We derived the gaseous sulfuric acid concentration proxy on the basis of currently accepted formation pathways of sulfuric acid in the atmosphere (R1-R3) (Finlayson-

Pitts and Pitts, 2000; Stockwell and Calvert, 1983):

$$OH + SO_2 \rightarrow HSO_3 \quad (R1)$$

$$HSO_3 + O_2 \rightarrow SO_3 + HO_2 \quad (R2)$$

$$SO_3 + 2H_2O \rightarrow H_2SO_4 + H_2O \quad (R3)$$

The reaction (R1) is the rate-limiting step of this formation pathway (Finlayson-Pitts and Pitts, 2000), so our proxy will consider the two major processes that determine the abundance of gaseous sulfuric acid: the formation of gaseous sulfuric acid from reactions between SO_2 and OH radicals, and the loss of gaseous sulfuric acid due to its condensation onto pre-existing particles (Dal Maso et al., 2002; Kulmala et al., 2012; Pirjola et al., 1999).

The rate of change of sulfuric acid concentration can be written as Eq. (4) (Mikkonen et al., 2011):

$$d[H_2SO_4]/dt = k \cdot [OH] \cdot [SO_2] - [H_2SO_4] \cdot CS \quad (4)$$

where k is a temperature-dependent reaction constant given by Eq. (5) (DeMore et al., 1997; Mikkonen et al., 2011).

$$k = \frac{A \cdot k_3}{(A + k_3)} \cdot exp\left\{k_5 \cdot \left[1 + log_{10}\left(\frac{A}{k_3}\right)^2\right]^{-1}\right\} \quad cm^3(molecule \cdot s)^{-1} \quad (5)$$

where $A = k_1 \cdot [M] \cdot (\frac{300}{T})^{k_2}$, $[M]$ represents the density of the air in molecule cm^{-3} as calculated by $0.101 \cdot (1.381 \cdot 10^{-23} \cdot T)^{-1}$, $k_1 = 4 \cdot 10^{-31}$, $k_2 = 3.3$, $k_3 = 2 \cdot 10^{-12}$ and $k_5 = -0.8$.

To simplify the calculation, the production and loss of sulfuric acid can be assumed to be at pseudo steady-state (Mikkonen et al., 2011; Petäjä et al., 2009). Then the sulfuric acid concentration can be written as Eq. (6).

$$[H_2SO_4] = k \cdot [OH] \cdot [SO_2] \cdot CS^{-1} \quad (6)$$

Atmospheric OH radical measurements represent a major challenge as well. Since

previous studies suggest that the OH radical concentration is strongly correlated with the intensity of UVB, [OH] could be replaced with UVB intensity in the proxy equation (Petäjä et al., 2009; Rohrer and Berresheim, 2006). Although photolysis of O_3 ($\lambda < 320\ nm$) and subsequent reactions with H_2O are considered to be the dominant source of OH radicals in the atmosphere (Logan et al., 1981), recent studies argue that photolysis of HONO ($\lambda < 400$ nm) is a potentially important OH radical formation pathway (Hendrick et al., 2014; Kleffmann, 2007; Su et al., 2011; Villena et al., 2011). Thus, we attempt to introduce both O_3 and HONO into the proxy equation and evaluate their effects on the concentration of OH radicals.

In practice, the exponents for variables in nonlinear fitting procedures are rarely equal to 1 (Mikkonen et al., 2011), so we replaced the factors x_i with $x_i^{w_i}$ in the proxy, where x_i can be an atmospheric variable such as UVB and [SO_2], and w_i defines x_i' weight in the proxy. Since k is a temperature-dependent reaction constant and varies within a 10 % range in the atmosphere temperature range of 267.6 - 292.6 K, *i.e.*, the actual atmospheric temperature variation in this study, we approximately regard k as a constant and use a new scaling factor k_0. This methodology has been used previously in the proxies of gaseous sulfuric acid in Hyytiälä, Southern Finland (Petäjä et al., 2009). As a result, the general proxy equation can be written as Eq. (7), with the UVB intensity, [SO_2], condensation sink (CS), [O_3], and [HONO] (or [NO_x]) as predictor variables:

$$[\boldsymbol{H_2SO_4}] = \boldsymbol{f}\left(\boldsymbol{k_0}\ , \boldsymbol{x_i^{\omega_i}}\right), \qquad \boldsymbol{x_i} = \boldsymbol{UVB}, [\boldsymbol{SO_2}], \boldsymbol{CS}, [\boldsymbol{O_3}], [\boldsymbol{HONO}] \ldots \quad (\mathbf{7})$$

The nonlinear curve-fitting procedures using iterative least square estimation for the proxies of gaseous sulfuric acid concentration based on Eq. (7) were performed by a custom-made MATLAB software. In addition to the correlation coefficient (R), relative error (RE) is used to evaluate the performance of proxies in the statistical analysis and can be written as Eq. (8).

$$\boldsymbol{RE} = \frac{\mathbf{1}}{\boldsymbol{n}} \cdot \sum_{\boldsymbol{i=1}}^{\boldsymbol{n}} \frac{|[\boldsymbol{H_2SO_4}]_{\boldsymbol{proxy,i}} - [\boldsymbol{H_2SO_4}]_{\boldsymbol{meas.,i}}|}{[\boldsymbol{H_2SO_4}]_{\boldsymbol{meas.,i}}} \qquad (\mathbf{8})$$

4 Results and discussion

4.1 General Characteristics of daytime sulfuric acid and atmospheric parameters

Table 1 summarizes the mean, median and 5-95 % percentiles of gaseous sulfuric

acid concentrations and other variables measured during the daytime of the campaign. The 5-95 % percentile ranges of the UVB intensity, [SO_2], [NO_x] and [O_3] were 0-0.45 W m^{-2}, 0.9-11.4 ppbv, 3.3-61.4 ppbv and 3.5-23.3 ppbv, respectively. Compared with the sites in the study by Mikkonen et al. (2011), Beijing was characterized with a factor of 1.4-13.1 higher mean [SO_2] but a factor of 3.4-5.4 lower mean [O_3]. The 5-95 % percentile range of CS in Beijing was 0.01-0.24 s^{-1}, which is about 10-100 times higher than corresponding value ranges in Europe and North America. The concentration of gaseous sulfuric acid during this campaign was $(2.2 - 10.0) \times 10^6$ molecule cm^{-3} in the 5-95 % percentile range, relatively similar to observed elsewhere around the world. A diurnal mean concentration of 0.74 ppbv for HONO was observed in this campaign, consistent with previous long-term HONO measurements of about 0.48-1.8 ppbv (averaged values) in winter in Beijing (Hendrick et al., 2014; Spataro et al., 2013; Wang et al., 2017), which is a factor of 4-10 higher than HONO concentrations measured in Europe (Alicke et al., 2002, 2003). In addition, Beijing is dry in winter with a mean ambient relative humidity of 28 % during the campaign.

4.2 Correlations between [H_2SO_4] and atmospheric variables

Table 2 summarizes the correlation coefficients between [H_2SO_4] and atmospheric variables using a Spearman-type correlation analysis. Clearly, the UVB intensity is an isolated variable that is independent of all the other variables but that imposes a positive influence on O_3 because of photochemical formation of ozone, and a negative influence on HONO because of HONO's photochemical degradation. The sulfuric acid concentration shows positive correlations with all the other variables. The correlation coefficients between [H_2SO_4] and [SO_2] and between [H_2SO_4] and UVB intensity are 0.74 and 0.46, respectively, which indicate that [SO_2] and UVB have important influences on the formation of atmospheric gaseous sulfuric acid. Accordingly, [O_3] and [HONO] show positive correlations with [H_2SO_4] because both O_3 and HONO could be precursors of OH radicals. Surprisingly, a high positive correlation coefficient (0.6) was found between [H_2SO_4] and CS, which is in contrast to the conventional thought that CS describes the loss of gaseous sulfuric acid molecules onto pre-existing particles and thus should show a negative correlation. CS correlates well with [SO_2] (r = 0.83) and [NO_x] (r = 0.77): a high CS value, as an indicator of atmospheric particle pollution, is thus usually accompanied with a high concentration of both SO_2 and NO_x in urban China, indicating co-emissions. A strong correlation between [HONO] and [NO_x] (r =

0.88) in our measurement is supported by the fact that HONO can be either heterogeneously formed by reactions of NO_2 on various surfaces (Calvert et al., 1994) or homogeneously formed by the gas phase NO + OH reaction, between which the former likely dominate for the daytime HONO production in urban Beijing (Liu et al., 2014).

Since the UVB intensity and [SO_2] have been reported as the dominating factors for the formation of sulfuric acid (Mikkonen et al., 2011; Petäjä et al., 2009), we further explored the relationship of the measured sulfuric acid concentrations with the UVB intensity and [SO_2] using the nonlinear curve-fitting method with a single variable. Figure 1a presents a scatter plot of [H_2SO_4] against the UVB intensity, color-coded by [SO_2]. A good correlation layering with [SO_2] is evident, indicating that the UVB intensity and [SO_2] together play an important role in the formation of sulfuric acid. A similar scatter plot (Figure 1b) of [H_2SO_4] against [SO_2], color-coded by the UVB intensity, leads to a similar conclusion.

4.3 Proxy construction

Similar to the non-linear proxies suggested by Mikkonen et al. (2011), we tested a number of proxies for gaseous sulfuric acid, listed in Table 3 with their respective fitting parameters and performance summarized in Table 4. The scatter plots of observed [H_2SO_4] *versus* predicted values given by proxies are presented in Fig. S1. In these proxies, the concentration of a gaseous species is in the unit of molecule cm^{-3}, the unit of the UVB intensity is W m^{-2}, the unit of CS is s^{-1}, and k_0 is a scaling factor.

The proxy N1 was built by using the UVB intensity and [SO_2] as the source terms and CS as the sink term, which follows the conventional idea of the H_2SO_4 formation and loss in the atmosphere. CS was then removed from this proxy to examine the performance of the proxy N2 that has the UVB intensity and [SO_2] as the only predictor variables. Since the formation of OH radicals in the atmosphere depends on precursors in addition to UVB, we further attempted to introduce the OH precursor term into the H_2SO_4 proxy. The proxies N3 and N4 were built by introducing O_3 as the only OH precursor to evaluate its influence on the formation of sulfuric acid. Furthermore, we added HONO as another potential precursor for OH radicals, resulting in the proxies N5 and N6. Lastly, the proxy N7 was built by replacing [HONO] with [NO_x] because firstly, HONO is not regularly measured, and secondly, a good linear correlation between [HONO] and [NO_x] was generally observed in the daytime during this

campaign, although higher [HONO]/[NO_x] ratios were observed in the morning due to the accumulation of HONO during the night (Figure 2). RH was not considered in the current study because a test by introducing RH into the proxies do not result in a significantly better performance, which is consistent with those conclusions in the Mikkonen et al. study (2011).

As shown in Table 4, the correlation coefficients are in the range of 0.83-0.86 and REs are in the range of 19.1-20.0 %. The exponents for the UVB intensity range from 0.13 to 0.16, and those for [SO_2] generally range from 0.38 to 0.41, except in case of the proxy N6 (b=0.33). The obtained exponent b for [SO_2] is significantly smaller than 1 unlike the assumption in Eq. (6), mainly because [SO_2] is also an indicator of air pollution that usually influences the sinks of both OH radicals and sulfuric acid. The exponent for [SO_2] ranged from 0.5 to 1.04 in the previous proxy study for European and North American sites (Mikkonen et al., 2011), including values from 0.48 to 0.69 in Atlanta, GA, USA, which was probably quite a polluted site because the measurements were conducted only 9 km away from a coal-fired power plant. The obtained value range of the exponent b for [SO_2] in our study is probably related to the urban nature of Beijing. The value of exponent c for CS in the proxy N1 is as low as 0.03, which either might be due to the covariance of CS and certain H_2SO_4 sources that cancels the dependence on CS, or it might indicate that CS is actually insufficient in regulating the H_2SO_4 concentration, as recently suggested by Kulmala et al. (2017). By comparing the proxies N1 and N2, we can see that CS plays a minor role because the exponents of [SO_2] and UVB, the overall correlation coefficient and the REs are almost identical with and without CS. We can see the negligible role of CS also when comparing the results of the proxies N3 and N4 where O_3 is considered. However, the role of CS becomes evident between the proxies N5 and N6 when HONO is introduced: the exponents of [SO_2], [O_3], and [HONO] significantly increased when taking into account the CS, suggesting that the covariance between HONO and CS can explain, at least partially, the close-to-zero exponent of CS in the proxies N1-N4. In addition, when [O_3] is introduced as the only precursor for OH radicals, minor improvements in the correlation coefficient and RE were obtained, as suggested by comparing the proxies N3 and N1. When both [O_3] and [HONO] were introduced as OH precursors in the proxies N5-N7, REs have noticeable improvements, and correlation coefficients improved slightly. Altogether, these observations suggest that it is crucial to introduce HONO into the proxy, both in our study and also likely for the previous work where

the exponent of CS is close-to-zero (Mikkonen et al., 2011).

Although so far the proxy N5 had the best fitting quality, it is impractical to explicitly include [HONO] because HONO measurements are very challenging. As shown in Fig. 2, [HONO] and [NO_x] tended to correlate linearly with each other in the daytime during this campaign, with a linearly fitted [HONO]/[NO_x] ratio of around 0.03 and a relative error of 0.42. Occasionally higher [HONO]/[NO_x] ratios could be seen in the morning, which might be due to the fact that HONO concentration could have an accumulation process during the nighttime and lead to a deviation from the steady state. Therefore, due to the good correlation, the proxy N7 replaces [HONO] by [NO_x], a more easily measured variable, and performs equally well with the proxy N5.

Clearly, the proxy N2 provides the simplest parameterization, but the proxies N5 and N7 result in the best fitting quality because of the introduction of [HONO]. Figure 3 presents the RE values for the proxies N2 and N7, respectively, as a function of linear bins of measured sulfuric acid concentrations. The performance of the proxy N7 is considerably better than that of the proxy N2 in the sulfuric acid concentration range of $(2.2 - 10) \times 10^6$ molecule cm^{-3}, which covers the 5-95% percentiles of sulfuric acid concentration in this study. In the worst scenario, RE of proxy N2 is 1.2 times as high as that of proxy N7, *e.g.*, REs are 16.75 % and 13.99 %, respectively, in the sulfuric acid concentration bin of $(4 - 5) \times 10^6$ molecule cm^{-3}, and 16.71 % and 14.42 %, respectively, in the bin of $(7 - 8) \times 10^6$ molecule cm^{-3}.

4.4 Comparison of measured and predicted [H_2SO_4]

A comparison between measured and predicted [H_2SO_4] was performed. Figure 4 includes calculated results from the proxies N2 and N7 as well as from a proxy constructed according to measurement in a boreal forest site, Finland, *i.e.*, Eq (1) (Petäjä et al., 2009). The measured daytime [H_2SO_4] on 10 March, 2018, was above 4×10^6 molecules cm^{-3} when averaged to a time resolution of 5 min. The predicted [H_2SO_4] using the proxies N2 and N7 both track the measured [H_2SO_4] pretty well, even when an unexpected dip in the sulfuric acid concentration was observed at around 10:00-11:00. The performance of the proxy N7 is better than that of proxy N2 during the entire day, consistent with our results in Fig. 3. The proxy by Petäjä et al. (2009) underestimated the concentrations of sulfuric acid by a factor of 20 or so, which can be attributed to the very different values of CS between Beijing and the boreal forest. The fact that $[H_2SO_4]_{\text{Petäjä } et\ al.}$ does not track the measured [H_2SO_4] even after including

a scaling factor indicates that proxies are site-specific and do not necessarily work well in locations other than where they have originally been developed for. In addition, the direct performance comparison between the proxy N2 and the proxy by Petäjä et al. (2009) indicates the importance of assigning exponential weights to variables in the nonlinear fitting procedures, which is consistent with results by Mikkonen et al. (2011).

5 Summary and conclusions

Sulfuric acid is a key precursor for atmospheric new particle formation. In this study, we constructed a number of proxies for gaseous sulfuric acid concentration according to our measurements in urban Beijing during the winter. According to the obtained proxies and their performance, the UVB intensity and [SO_2] were the dominant influencing factors. Hence, the simplest proxy (Proxy N2) only involves UVB intensity and [SO_2] as shown by Eq. (9). The units of [H_2SO_4] and [SO_2] are molecule cm^{-3}, and the unit of UVB is W m^{-2}.

$$[\boldsymbol{H_2SO_4}] = \mathbf{280.05} \cdot \boldsymbol{UVB}^{\mathbf{0.14}} \cdot [\boldsymbol{SO_2}]^{\mathbf{0.40}} \quad (\mathbf{9})$$

For a comprehensive consideration of the formation pathways of OH radicals, [O_3] and [HONO] as well as CS should be included (Proxy N5), as shown by Eq. (10). The units of [H_2SO_4], [SO_2], [O_3] and [HONO] are molecule cm^{-3}, the unit of UVB is W m^{-2}, and the unit of CS is s^{-1}.

$$[\boldsymbol{H_2SO_4}] = \mathbf{0.0072} \cdot \boldsymbol{UVB}^{\mathbf{0.15}} \cdot [\boldsymbol{SO_2}]^{\mathbf{0.41}} \cdot \boldsymbol{CS}^{\mathbf{-0.17}} \cdot ([\boldsymbol{O_3}]^{\mathbf{0.36}} + [\boldsymbol{HONO}]^{\mathbf{0.38}}) \quad (\mathbf{10})$$

Since HONO measurements are not a regular practice, we can further replace [HONO] with [NO_x], shown in Eq. (11), which can be justified by the strong linear correlation between [HONO] and [NO_x] observed in this study. The units of [H_2SO_4], [SO_2], [O_3] and [NO_x] are molecule cm^{-3}, the unit of UVB is W m^{-2}, and the unit of CS is s^{-1}.

$$[\boldsymbol{H_2SO_4}] = \mathbf{0.0013} \cdot \boldsymbol{UVB}^{\mathbf{0.13}} \cdot [\boldsymbol{SO_2}]^{\mathbf{0.40}} \cdot \boldsymbol{CS}^{\mathbf{-0.17}} \cdot ([\boldsymbol{O_3}]^{\mathbf{0.44}} + [\boldsymbol{NO_x}]^{\mathbf{0.41}}) \quad (\mathbf{11})$$

We consider this last proxy more reasonable than the others due to the following reasons:

first, it makes the equation physically meaningful as the CS starts to be involved as a sink term, and second, the RE was reduced considerably compared with the other proxies. Overall, this suggests that the photolysis of O_3 and HONO are both important OH sources in urban Beijing.

As a summary, we recommend using the simplest proxy (proxy N2 as shown in Eq. (9)) and a more accurate proxy (Proxy N7 as shown in Eq. (11)) for calculating daytime gaseous sulfuric acid concentrations in the urban Beijing atmosphere. It is clear that the current proxies are based on only a month-long campaign of sulfuric acid measurements in urban Beijing during winter. Given the dramatic reduction in the concentration of SO_2 in recent years (Wang et al., 2018) and the strong dependence of calculated [H_2SO_4] on [SO_2], the performance of the proxies in the past and future years remain to be evaluated. Furthermore, the proxies might be site-specific and season-specific. Since the proxies were derived with atmospheric parameters in winter, in urban Beijing, the exponents for atmospheric variables in the proxy could have different values for other cities or other seasons. Thus, the proxies in this study should be further tested before their application to other Chinese megacities or other seasons.

Author contributions

LW designed this study. YL (Yiqun Lu), CY, YF, YC, YL (Yiliang Liu), GY, YW, YZ, RY, RB and CD conducted the field campaign. YL (Yiqun Lu) analyzed data with contributions from LW and all the other co-authors. YL (Yiqun Lu) and LW wrote the manuscript with contributions from all the other co-authors.

Acknowledgement

This study was financially supported by the National Key R&D Program of China (2017YFC0209505), and the National Natural Science Foundation of China (41575113, 91644213).

References

Acker, K., Möller, D., Auel, R., Wieprecht, W. and Kalaß, D.: Concentrations of nitrous acid, nitric acid, nitrite and nitrate in the gas and aerosol phase at a site in the emission zone during ESCOMPTE 2001 experiment, Atmos. Res., 74(1–4), 507–524, doi:10.1016/j.atmosres.2004.04.009, 2005.

Alicke, B., Platt, U. and Stutz, J.: Impact of nitrous acid photolysis on the total hydroxyl radical budget during the Limitation of Oxidant Production/Pianura Padana Produzione di Ozono study in Milan, J. Geophys. Res. Atmos., 107(22), doi:10.1029/2000JD000075, 2002.

Alicke, B., Geyer., A., Hofzumahaus, A., Holland, F., Konrad, S., Patz, H. W., Schafer, J., Stutz, J., Volz-Thomas, A. and Platt, U.: OH formation by HONO photolysis during the BERLIOZ experiment, J. Geophys. Res., 108(D4), 8247, doi:10.1029/2001JD000579, 2003.

Almeida, J., Schobesberger, S., Kürten, A., Ortega, I. K., Kupiainen-Määttä, O., Praplan, A. P., Adamov, A., Amorim, A., Bianchi, F., Breitenlechner, M., David, A., Dommen, J., Donahue, N. M., Downard, A., Dunne, E., Duplissy, J., Ehrhart, S., Flagan, R. C., Franchin, A., Guida, R., Hakala, J., Hansel, A., Heinritzi, M., Henschel, H., Jokinen, T., Junninen, H., Kajos, M., Kangasluoma, J., Keskinen, H., Kupc, A., Kurtén, T., Kvashin, A. N., Laaksonen, A., Lehtipalo, K., Leiminger, M., Leppä, J., Loukonen, V., Makhmutov, V., Mathot, S., McGrath, M. J., Nieminen, T., Olenius, T., Onnela, A., Petäjä, T., Riccobono, F., Riipinen, I., Rissanen, M., Rondo, L., Ruuskanen, T., Santos, F. D., Sarnela, N., Schallhart, S., Schnitzhofer, R., Seinfeld, J. H., Simon, M., Sipilä, M., Stozhkov, Y., Stratmann, F., Tomé, A., Tröstl, J., Tsagkogeorgas, G., Vaattovaara, P., Viisanen, Y., Virtanen, A., Vrtala, A., Wagner, P. E., Weingartner, E., Wex, H., Williamson, C., Wimmer, D., Ye, P., Yli-Juuti, T., Carslaw, K. S., Kulmala, M., Curtius, J., Baltensperger, U., Worsnop, D. R., Vehkamäki, H. and Kirkby, J.: Molecular understanding of sulphuric acid-amine particle nucleation in the atmosphere, Nature, 502(7471), 359–363, doi:10.1038/nature12663, 2013.

Arnold, F. and Fabian, R.: First measurements of gas phase sulphuric acid in the stratosphere, Nature, 283(3), 55–57, 1980.

Aumont, B., Chervier, F. and Laval, S.: Contribution of HONO sources to the $NO_x/HO_x/O_3$ chemistry in the polluted boundary layer, Atmos. Environ., 37(4), 487–498, doi:10.1016/S1352-2310(02)00920-2, 2003.

Benson, D. R., Young, L. H., Kameel, F. R. and Lee, S. H.: Laboratory-measured nucleation rates of sulfuric acid and water binary homogeneous nucleation from the SO_2 + OH reaction, Geophys. Res. Lett., 35(11), 1–6, doi:10.1029/2008GL033387, 2008.

Berresheim, H., Elste, T., Plass-Dülmer, C., Eisele, F. L. and Tanner, D. J.: Chemical ionization mass spectrometer for long-term measurements of atmospheric OH and H_2SO_4, Int. J. Mass Spectrom., 202(1–3), 91–109, doi:10.1016/S1387-3806(00)00233-5, 2000.

Bianchi, F., Tröstl, J., Junninen, H., Frege, C., Henne, S., Hoyle, C. R., Molteni, U., Herrmann, E., Adamov, A., Bukowiecki, N., Chen, X., Duplissy, J., Gysel, M., Hutterli, M., Kangasluoma, J., Kontkanen, J., Kurten, A., Manninen, H. E., Munch, S., Perakylä, O., Petäjä, T., Rondo, L., Williamson, C., Weingartner, E., Curtius, J., Worsnop, D. R., Kulmala, M., Dommen, J. and Baltensperger, U.: New particle formation in the free troposphere: A question of chemistry and timing, Science, 352(6289), 1109–1112, doi:10.1126/science.aad5456, 2016.

520 Boy, M., Mogensen, D., Smolander, S., Zhou, L., Nieminen, T., Paasonen, P., Plass-Dülmer, C.,
521 Sipilä, M., Petäjä, T., Mauldin, L., Berresheim, H. and Kulmala, M.: Oxidation of SO_2 by
522 stabilized Criegee intermediate (sCI) radicals as a crucial source for atmospheric sulfuric acid
523 concentrations, Atmos. Chem. Phys., 13(7), 3865–3879, doi:10.5194/acp-13-3865-2013, 2013.
524 Cai, R., Chen, D. R., Hao, J. and Jiang, J.: A miniature cylindrical differential mobility analyzer for
525 sub-3 nm particle sizing, J. Aerosol Sci., 106(September 2016), 111–119,
526 doi:10.1016/j.jaerosci.2017.01.004, 2017.
527 Calvert, J. G., Yarwood, G. and Dunker, A. M.: An evaluation of the mechanism of nitrous acid
528 formation in the urban atmosphere, Res. Chem. Intermed., 20(3–5), 463–502,
529 doi:10.1163/156856794X00423, 1994.
530 Chen, M., Titcombe, M., Jiang, J., Jen, C., Kuang, C., Fischer, M. L. and Eisele, F. L.: Acid-base
531 chemical reaction model for nucleation rates in the polluted atmospheric boundary layer, Proc.
532 Natl. Acad. Sci., 109(46), 18713–18718, doi:10.1073/pnas.1210285109, 2012.
533 Crutzen, P. J. and Zimmermann, P. H.: The changing photochemistry of the troposphere, Tellus,
534 43AB(December), 136–151, doi:10.3402/tellusb.v43i4.15397, 1991.
535 Dal Maso, M., Kulmala, M., Lehtinen, K. E. J., Mäkelä, J. M., Aalto, P. and O'Dowd, C. D.:
536 Condensation and coagulation sinks and formation of nucleation mode particles in coastal and
537 boreal forest boundary layers, J. Geophys. Res. Atmos., 107(19), doi:10.1029/2001JD001053,
538 2002.
539 DeMore, W. B., Sander, S. P., Golden, D. M., Hampson, R. F., Kurylo, M. J., Howard, C. J.,
540 Ravishankara, A. R., Kolb, C. E. and Molina, M. J.: Chemical kinetics and photochemical data
541 for use in stratospheric modeling, JPL Publ., 97–4(12), 278, doi:10.1002/kin.550171010, 1997.
542 Dunn, M. J., Baumgardner, D., Castro, T., Mcmurry, P. H. and Smith, J. N.: Measurements of
543 Mexico City nanoparticle size distributions : Observations of new particle formation and
544 growth, Geophys. Res. Lett., 31, L10102, doi:10.1029/2004GL019483, 2004.
545 Duplissy, J., Merikanto, J., Franchin, A., Tsagkogeorgas, G., Kangasluoma, J., Wimmer, D.,
546 Vuollekoski, H., Schobesberger, S., Lehtipalo, K., Flagan, R. C., Brus, D., Donahue, N. M.,
547 Vehkamäki, H., Almeida, J., Amorim, A., Barmet, P., Bianchi, F., Breitenlechner, M., Dunne,
548 E. M., Guida, R., Henschel, H., Junninen, H., Kirkby, J., Kürten, A., Kupc, A., Määttänen, A.,
549 Makhmutov, V., Mathot, S., Nieminen, T., Onnela, A., Praplan, A. P., Riccobono, F., Rondo,
550 L., Steiner, G., Tome, A., Walther, H., Baltensperger, U., Carslaw, K. S., Dommen, J., Hansel,
551 A., Petäjä, T., Sipilä, M., Stratmann, F., Vrtala, A., Wagner, P. E., Worsnop, D. R., Curtius, J.
552 and Kulmala, M.: Effect of dimethylamine on the gas phase sulfuric acid concentration
553 measured by Chemical Ionization Mass Spectrometry, J. Geophys. Res. Atmos., 1752–1775,
554 doi:10.1002/2015JD023538.Effect, 2016.
555 Eisele, F. L. and Tanner, D. J.: Measurement of the gas phase concentration of H_2SO_4 and methane
556 sulfonic acid and estimates of H2SO4 production and loss in the atmosphere, J. Geophys. Res.
557 Atmos., 98(D5), 9001–9010, doi:10.1029/93JD00031, 1993.
558 Elshorbany, Y. F., Kurtenbach, R., Wiesen, P., Lissi, E., Rubio, M., Villena, G., Gramsch, E.,
559 Rickard, A. R., Pilling, M. J. and Kleffmann, J.: Oxidation capacity of the city air of Santiago,
560 Chile, Atmos. Chem. Phys., doi:10.5194/acp-9-2257-2009, 2009.
561 Finlayson-Pitts, B. J. and Pitts, J. N.: Acid Deposition: Formation and Fates of Inorganic and

562 Organic Acids in the Troposphere, in Chemistry of the Upper and Lower Atmosphere: Theory,
563 Experiments, and Applications, p. 969, Academic Press, San Diego., 2000.
564 Fuchs, N. A. and Sutugin, A. G.: Highly dispersed aerosols, in Topics in Current Aerosol Research,
565 edited by G. M. HIDY and J. R. BROCK, p. 1, Pergamon., 1971.
566 Gopalakrishnan, R. and Hogan Jr., C. J.: Determination of the Transition Regime Collision Kernel
567 from Mean First Passage Times Determination of the Transition Regime Collision Kernel from
568 Mean First Passage Times, Aerosol Sci. Technol. ISSN, 45, 1499–1509,
569 doi:10.1080/02786826.2011.601775, 2011.
570 Hendrick, F., Clémer, K., Wang, P., De Mazière, M., Fayt, C., Gielen, C., Hermans, C., Ma, J. Z.,
571 Pinardi, G., Stavrakou, T., Vlemmix, T. and Van Roozendael, M.: Four years of ground-based
572 MAX-DOAS observations of HONO and NO_2 in the Beijing area, Atmos. Chem. Phys., 14(2),
573 765–781, doi:10.5194/acp-14-765-2014, 2014.
574 Herrmann, E., Ding, A. J., Kerminen, V. M., Petäjä, T., Yang, X. Q., Sun, J. N., Qi, X. M., Manninen,
575 H., Hakala, J., Nieminen, T., Aalto, P. P., Kulmala, M. and Fu, C. B.: Aerosols and nucleation
576 in eastern China: First insights from the new SORPES-NJU station, Atmos. Chem. Phys., 14(4),
577 2169–2183, doi:10.5194/acp-14-2169-2014, 2014.
578 Jen, C. N., McMurry, P. H. and Hanson, D. R.: Stabilization of sulfuric acid dimers by ammonia,
579 methylamine, dimethylamine, and trimethylamine, J. Geophys. Res. Atmos., 7502–7514,
580 doi:10.1002/2014JD021592.Received, 2014.
581 Jiang, J., Zhao, J., Chen, M., Eisele, F. L., Scheckman, J., Williams, B. J., Kuang, C. and McMurry,
582 P. H.: First measurements of neutral atmospheric cluster and 1-2 nm particle number size
583 distributions during nucleation events, Aerosol Sci. Technol., 45(4),
584 doi:10.1080/02786826.2010.546817, 2011.
585 Jokinen, T., Sipilä, M., Junninen, H., Ehn, M., Lönn, G., Hakala, J., Petäjä, T., Mauldin, R. L.,
586 Kulmala, M. and Worsnop, D. R.: Atmospheric sulphuric acid and neutral cluster
587 measurements using CI-APi-TOF, Atmos. Chem. Phys., 12(9), 4117–4125, doi:10.5194/acp-
588 12-4117-2012, 2012.
589 Junninen, H., Ehn, M., Petäjä, Luosujärvi, L., Kotiaho, T., Kostiainen, R., Rohner, U., Gonin, M.,
590 Fuhrer, K., Kulmala, M. and Worsnop, D. R.: A high-resolution mass spectrometer to measure
591 atmospheric ion composition, Atmos. Meas. Tech., 3(4), 1039–1053, doi:10.5194/amt-3-1039-
592 2010, 2010.
593 Kerminen, V.: Atmospheric new particle formation and growth : review of field observations,
594 Environ. Res. Lett., 13, 103003, 2018.
595 Kerminen, V. M., Petäjä, T., Manninen, H. E., Paasonen, P., Nieminen, T., Sipilä, M., Junninen, H.,
596 Ehn, M., Gagné, S., Laakso, L., Riipinen, I., Vehkamäki, H., Kurtén, T., Ortega, I. K., Dal
597 Maso, M., Brus, D., Hyvärinen, A., Lihavainen, H., Leppä, J., Lehtinen, K. E. J., Mirme, A.,
598 Mirme, S., Hõrrak, U., Berndt, T., Stratmann, F., Birmili, W., Wiedensohler, A., Metzger, A.,
599 Dommen, J., Baltensperger, U., Kiendler-Scharr, A., Mentel, T. F., Wildt, J., Winkler, P. M.,
600 Wagner, P. E., Petzold, A., Minikin, A., Plass-Dülmer, C., Pöschl, U., Laaksonen, A. and
601 Kulmala, M.: Atmospheric nucleation: Highlights of the EUCAARI project and future
602 directions, Atmos. Chem. Phys., 10(22), 10829–10848, doi:10.5194/acp-10-10829-2010, 2010.
603 Kirkby, J., Curtius, J., Almeida, J., Dunne, E., Duplissy, J., Ehrhart, S., Franchin, A., Gagné, S.,

Ickes, L., Kürten, A., Kupc, A., Metzger, A., Riccobono, F., Rondo, L., Schobesberger, S., Tsagkogeorgas, G., Wimmer, D., Amorim, A., Bianchi, F., Breitenlechner, M., David, A., Dommen, J., Downard, A., Ehn, M., Flagan, R. C., Haider, S., Hansel, A., Hauser, D., Jud, W., Junninen, H., Kreissl, F., Kvashin, A., Laaksonen, A., Lehtipalo, K., Lima, J., Lovejoy, E. R., Makhmutov, V., Mathot, S., Mikkilä, J., Minginette, P., Mogo, S., Nieminen, T., Onnela, A., Pereira, P., Petäjä, T., Schnitzhofer, R., Seinfeld, J. H., Sipilä, M., Stozhkov, Y., Stratmann, F., Tomé, A., Vanhanen, J., Viisanen, Y., Vrtala, A., Wagner, P. E., Walther, H., Weingartner, E., Wex, H., Winkler, P. M., Carslaw, K. S., Worsnop, D. R., Baltensperger, U. and Kulmala, M.: Role of sulphuric acid, ammonia and galactic cosmic rays in atmospheric aerosol nucleation, Nature, 476, 429 [online] Available from: http://dx.doi.org/10.1038/nature10343, 2011.

Kleffmann, J.: Daytime sources of nitrous acid (HONO) in the atmospheric boundary layer, ChemPhysChem, 8(8), 1137–1144, doi:10.1002/cphc.200700016, 2007.

Korhonen, P., Kulmala, M., Laaksonen, A., Viisanen, Y., McGraw, R. and Seinfeld, J. H.: Ternary nucleation of H_2SO_4, NH_3, and H_2O in the atmosphere, J. Geophys. Res., doi:10.1029/1999JD900784, 1999.

Kuang, C., McMurry, P. H., McCormick, A. V. and Eisele, F. L.: Dependence of nucleation rates on sulfuric acid vapor concentration in diverse atmospheric locations, J. Geophys. Res. Atmos., 113(10), 1–9, doi:10.1029/2007JD009253, 2008.

Kuang, C., Chen, M., Zhao, J., Smith, J., Mcmurry, P. H. and Wang, J.: Size and time-resolved growth rate measurements of 1 to 5nm freshly formed atmospheric nuclei, Atmos. Chem. Phys., 12, 3573–3589, doi:10.5194/acp-12-3573-2012, 2012.

Kulmala, M. and Kerminen, V. M.: On the formation and growth of atmospheric nanoparticles, Atmos. Res., 90(2–4), 132–150, doi:10.1016/j.atmosres.2008.01.005, 2008.

Kulmala, M., Petäjä, T., Nieminen, T., Sipilä, M., Manninen, H. E., Lehtipalo, K., Dal Maso, M., Aalto, P. P., Junninen, H., Paasonen, P., Riipinen, I., Lehtinen, K. E. J., Laaksonen, A. and Kerminen, V.-M.: Measurement of the nucleation of atmospheric aerosol particles, Nat. Protoc., 7(9), 1651–1667, doi:10.1038/nprot.2012.091, 2012.

Kulmala, M., Kontkanen, J., Junninen, H., Lehtipalo, K., Manninen, H. E., Nieminen, T., Petäjä, T., Sipilä, M., Schobesberger, S., Rantala, P., Franchin, A., Jokinen, T., Järvinen, E., Äijälä, M., Kangasluoma, J., Hakala, J., Aalto, P. P., Paasonen, P., Mikkilä, J., Vanhanen, J., Aalto, J., Hakola, H., Makkonen, U., Ruuskanen, T., Mauldin, R. L., Duplissy, J., Vehkamäki, H., Bäck, J., Kortelainen, A., Riipinen, I., Kurtén, T., Johnston, M. V., Smith, J. N., Ehn, M., Mentel, T. F., Lehtinen, K. E. J., Laaksonen, A., Kerminen, V. M. and Worsnop, D. R.: Direct observations of atmospheric aerosol nucleation, Science, 339(6122), 943–946, doi:10.1126/science.1227385, 2013.

Kulmala, M., Kerminen, V.-M., Petäjä, T., Ding, A. J. and Wang, L.: Atmospheric gas-to-particle conversion: why NPF events are observed in megacities?, Faraday Discuss., 200(0), 271–288, doi:10.1039/C6FD00257A, 2017.

Kürten, A., Rondo, L., Ehrhart, S. and Curtius, J.: Calibration of a chemical ionization mass spectrometer for the measurement of gaseous sulfuric acid, J. Phys. Chem. A, 116(24), 6375–6386, doi:10.1021/jp212123n, 2012.

Kürten, A., Jokinen, T., Simon, M., Sipilä, M., Sarnela, N., Junninen, H., Adamov, A., Almeida, J.,

Amorim, A., Bianchi, F., Breitenlechner, M., Dommen, J., Donahue, N. M., Duplissy, J., Ehrhart, S., Flagan, R. C., Franchin, A., Hakala, J., Hansel, A., Heinritzi, M., Hutterli, M., Kangasluoma, J., Kirkby, J., Laaksonen, A., Lehtipalo, K., Leiminger, M., Makhmutov, V., Mathot, S., Onnela, A., Petäjä, T., Praplan, A. P., Riccobono, F., Rissanen, M. P., Rondo, L., Schobesberger, S., Seinfeld, J. H., Steiner, G., Tomé, A., Tröstl, J., Winkler, P. M., Williamson, C., Wimmer, D., Ye, P., Baltensperger, U., Carslaw, K. S., Kulmala, M., Worsnop, D. R. and Curtius, J.: Neutral molecular cluster formation of sulfuric acid-dimethylamine observed in real time under atmospheric conditions, Proc. Natl. Acad. Sci., 111(42), 15019–15024, doi:10.1073/pnas.1404853111, 2014.

Kürten, A., Münch, S., Rondo, L., Bianchi, F., Duplissy, J., Jokinen, T., Junninen, H., Sarnela, N., Schobesberger, S., Simon, M., Sipilä, M., Almeida, J., Amorim, A., Dommen, J., Donahue, N. M., Dunne, E. M., Flagan, R. C., Franchin, A., Kirkby, J., Kupc, A., Makhmutov, V., Petäjä, T., Praplan, A. P., Riccobono, F., Steiner, G., Tomé, A., Tsagkogeorgas, G., Wagner, P. E., Wimmer, D., Baltensperger, U., Kulmala, M., Worsnop, D. R. and Curtius, J.: Thermodynamics of the formation of sulfuric acid dimers in the binary (H_2SO_4-H_2O) and ternary (H_2SO_4-H_2O-NH_3) system, Atmos. Chem. Phys., 15(18), 10701–10721, doi:10.5194/acp-15-10701-2015, 2015.

Kurtén, T., Petäjä, T., Smith, J., Ortega, I. K., Sipilä, M., Junninen, H., Ehn, M., Vehkamäki, H., Mauldin, L., Worsnop, D. R. and Kulmala, M.: The effect of H_2SO_4-amine clustering on chemical ionization mass spectrometry (CIMS) measurements of gas-phase sulfuric acid, Atmos. Chem. Phys., 11(6), 3007–3019, doi:10.5194/acp-11-3007-2011, 2011.

Li, X., Brauers, T., Häseler, R., Bohn, B., Fuchs, H., Hofzumahaus, A., Holland, F., Lou, S., Lu, K. D., Rohrer, F., Hu, M., Zeng, L. M., Zhang, Y. H., Garland, R. M., Su, H., Nowak, A., Wiedensohler, A., Takegawa, N., Shao, M. and Wahner, A.: Exploring the atmospheric chemistry of nitrous acid (HONO) at a rural site in Southern China, Atmos. Chem. Phys., 12(3), 1497–1513, doi:10.5194/acp-12-1497-2012, 2012.

Liu, J., Jiang, J., Zhang, Q., Deng, J. and Hao, J.: A spectrometer for measuring particle size distributions in the range of 3 nm to 10 μm, Front. Environ. Sci. Eng., 10(1), 63–72, doi:10.1007/s11783-014-0754-x, 2016.

Liu, Z., Wang, Y., Costabile, F., Amoroso, A., Zhao, C., Huey, L. G., Stickel, R., Liao, J. and Zhu, T.: Evidence of Aerosols as a Media for Rapid Daytime HONO Production over China, Environ. Sci. Technol., 48(24), 14386–14391, doi:10.1021/es504163z, 2014.

Logan, J. A., Prather, M. J., Wofsy, S. C. and Mcelroy, M. B.: Tropospheric chemistry: A global perspective, J. Geophys. Res., 86(C8), 7210–7254, doi:10.1029/JC086iC08p07210, 1981.

Mauldin, R. L., Berndt, T., Sipilä, M., Paasonen, P., Petäjä, T., Kim, S., Kurtén, T., Stratmann, F., Kerminen, V. M. and Kulmala, M.: A new atmospherically relevant oxidant of sulphur dioxide, Nature, 488(7410), 193–196, doi:10.1038/nature11278, 2012.

Mikkonen, S., Romakkaniemi, S., Smith, J. N., Korhonen, H., Petäjä, T., Plass-Duelmer, C., Boy, M., McMurry, P. H., Lehtinen, K. E. J., Joutsensaari, J., Hamed, A., Mauldin, R. L., Birmili, W., Spindler, G., Arnold, F., Kulmala, M. and Laaksonen, A.: A statistical proxy for sulphuric acid concentration, Atmos. Chem. Phys., 11(21), 11319–11334, doi:10.5194/acp-11-11319-2011, 2011.

Nieminen, T., Lehtinen, K. E. J. and Kulmala, M.: Sub-10 nm particle growth by vapor condensation-effects of vapor molecule size and particle thermal speed, Atmos. Chem. Phys., 10(20), 9773–9779, doi:10.5194/acp-10-9773-2010, 2010.

Paasonen, P., Nieminen, T., Asmi, E., Manninen, H. E., Petäjä, T., Plass-Dülmer, C., Flentje, H., Birmili, W., Wiedensohler, A., Hõrrak, U., Metzger, A., Hamed, A., Laaksonen, A., Facchini, M. C., Kerminen, V. M. and Kulmala, M.: On the roles of sulphuric acid and low-volatility organic vapours in the initial steps of atmospheric new particle formation, Atmos. Chem. Phys., 10(22), 11223–11242, doi:10.5194/acp-10-11223-2010, 2010.

Petäjä, T., Mauldin, R. L., Kosciuch, E., McGrath, J., Nieminen, T., Paasonen, P., Boy, M., Adamov, A., Kotiaho, T. and Kulmala, M.: Sulfuric acid and OH concentrations in a boreal forest site, Atmos. Chem. Phys., 9(19), 7435–7448, doi:10.5194/acp-9-7435-2009, 2009.

Petäjä, T., Sipilä, M., Paasonen, P., Nieminen, T., Kurtén, T., Ortega, I. K., Stratmann, F., Vehkamäki, H., Berndt, T. and Kulmala, M.: Experimental observation of strongly bound dimers of sulfuric acid: Application to nucleation in the atmosphere, Phys. Rev. Lett., 106(22), 1–4, doi:10.1103/PhysRevLett.106.228302, 2011.

Pirjola, L., Kulmala, M., Wilck, M., Bischoff, A., Stratmann, F. and Otto, E.: Formation of sulphuric acid aerosols and cloud condensation nuclei: An expression for significant nucleation and model comparison, J. Aerosol Sci., doi:10.1016/S0021-8502(98)00776-9, 1999.

Rohrer, F. and Berresheim, H.: Strong correlation between levels of tropospheric hydroxyl radicals and solar ultraviolet radiation, Nature, 442(7099), 184–187, doi:10.1038/nature04924, 2006.

Sipilä, M., Berndt, T., Petäjä, T., Brus, D., Vanhanen, J., Stratmann, F., Patokoski, J., Mauldin, R. L., Hyvärinen, A. P., Lihavainen, H. and Kulmala, M.: The role of sulfuric acid in atmospheric nucleation, Science, 327(5970), 1243–1246, doi:10.1126/science.1180315, 2010.

Smith, J. N., Dunn, M. J., Vanreken, T. M., Iida, K., Stolzenburg, M. R., Mcmurry, P. H. and Huey, L. G.: Chemical composition of atmospheric nanoparticles formed from nucleation in Tecamac , Mexico : Evidence for an important role for organic species in nanoparticle growth, Geophys. Res. Lett., 35, L04808, doi:10.1029/2007GL032523, 2008.

Spataro, F., Ianniello, A., Esposito, G., Allegrini, I., Zhu, T. and Hu, M.: Occurrence of atmospheric nitrous acid in the urban area of Beijing (China), Sci. Total Environ., 447, 210–224, doi:10.1016/j.scitotenv.2012.12.065, 2013.

Stockwell, W. R. and Calvert, J. G.: The mechanism of the HO-SO_2 reaction, Atmos. Environ., 17(11), 2231–2235, doi:10.1016/0004-6981(83)90220-2, 1983.

Su, H., Cheng, Y., Oswald, R., Behrendt, T., Trebs, I., Meixner, F. X., Andreae, M. O., Cheng, P., Zhang, Y. and Pöschl, U.: Soil nitrite as a source of atmospheric HONO and OH radicals, Science, 333(6049), 1616–1618, doi:10.1126/science.1207687, 2011.

Tong, S., Hou, S., Zhang, Y., Chu, B., Liu, Y., He, H., Zhao, P. and Ge, M.: Exploring the nitrous acid (HONO) formation mechanism in winter Beijing: Direct emissions and heterogeneous production in urban and suburban areas, Faraday Discuss., 189, 213–230, doi:10.1039/c5fd00163c, 2016.

Villena, G., Wiesen, P., Cantrell, C. A., Flocke, F., Fried, A., Hall, S. R., Hornbrook, R. S., Knapp, D., Kosciuch, E., Mauldin, R. L., McGrath, J. A., Montzka, D., Richter, D., Ullmann, K., Walega, J., Weibring, P., Weinheimer, A., Staebler, R. M., Liao, J., Huey, L. G. and Kleffmann,

730 J.: Nitrous acid (HONO) during polar spring in Barrow, Alaska: A net source of OH radicals?,
731 J. Geophys. Res. Atmos., 116(24), 1–12, doi:10.1029/2011JD016643, 2011.
732 Wang, J., Zhang, X., Guo, J., Wang, Z. and Zhang, M.: Observation of nitrous acid (HONO) in
733 Beijing, China: Seasonal variation, nocturnal formation and daytime budget, Sci. Total
734 Environ., 587–588, 350–359, doi:10.1016/j.scitotenv.2017.02.159, 2017.
735 Wang, M., Zhu, T., Zhang, J. P., Zhang, Q. H., Lin, W. W., Li, Y. and Wang, Z. F.: Using a mobile
736 laboratory to characterize the distribution and transport of sulfur dioxide in and around Beijing,
737 Atmos. Chem. Phys., 11(22), 11631–11645, doi:10.5194/acp-11-11631-2011, 2011a.
738 Wang, Z., Zheng, F., Zhang, W. and Wang, S.: Analysis of SO2 Pollution Changes of Beijing-
739 Tianjin-Hebei Region over China Based on OMI Observations from 2006 to 2017, Adv.
740 Meteorol., 2018, Article ID 8746068, 2018.
741 Wang, Z. B., Hu, M., Yue, D. L., Zheng, J., Zhang, R. Y., Wiedensohler, A., Wu, Z. J., Nieminen,
742 T. and Boy, M.: Evaluation on the role of sulfuric acid in the mechanisms of new particle
743 formation for Beijing case, Atmos. Chem. Phys., 11(24), 12663–12671, doi:10.5194/acp-11-
744 12663-2011, 2011b.
745 Weber, R. J., Marti, J. J., McMurry, P. H., Eisele, F. L., Tanner, D. J. and Jefferson, a.:
746 Measurements of new particle formation and ultrafine particle growth rates at a clean
747 continental site, J. Geophys. Res. Atmos., 102, 4375–4385, doi:10.1029/96JD03656, 1997.
748 Wu, F., Xie, P., Li, A., Mou, F., Chen, H., Zhu, Y., Zhu, T., Liu, J. and Liu, W.: Investigations of
749 temporal and spatial distribution of precursors SO_2 and NO_2 vertical columns in the North
750 China Plain using mobile DOAS, Atmos. Chem. Phys., 18, 1535–1554, doi:10.5194/acp-2017-
751 719, 2017.
752 Wu, Z., Hu, M., Liu, S., Wehner, B., Bauer, S., Ma ßling, A., Wiedensohler, A., Petäjä, T., Dal
753 Maso, M. and Kulmala, M.: New particle formation in Beijing, China: Statistical analysis of a
754 1-year data set, J. Geophys. Res., 112(D9), D09209, doi:10.1029/2006JD007406, 2007.
755 Xiao, S., Wang, M. Y., Yao, L., Kulmala, M., Zhou, B., Yang, X., Chen, J. M., Wang, D. F., Fu, Q.
756 Y., Worsnop, D. R. and Wang, L.: Strong atmospheric new particle formation in winter in
757 urban Shanghai, China, Atmos. Chem. Phys., 15(4), 1769–1781, doi:10.5194/acp-15-1769-
758 2015, 2015.
759 Yao, L., Garmash, O., Bianchi, F., Zheng, J., Yan, C., Kontkanen, J., Junninen, H., Mazon, S. B.,
760 Ehn, M., Paasonen, P., Sipilä, M., Wang, M., Wang, X., Xiao, S., Chen, H., Lu, Y., Zhang, B.,
761 Wang, D., Fu, Q., Geng, F., Li, L., Wang, H., Qiao, L., Yang, X., Chen, J., Kerminen, V.-M.,
762 Petäjä, T., Worsnop, D. R., Kulmala, M. and Wang, L.: Atmospheric new particle formation
763 from sulfuric acid and amines in a Chinese megacity, Science, 361(6399), 278–281,
764 doi:10.1126/science.aao4839, 2018.
765 Yue, D., Hu, M., Wu, Z., Wang, Z., Guo, S., Wehner, B., Nowak, A., Achtert, P., Wiedensohler, A.,
766 Jung, J., Kim, Y. J. and Liu, S.: Characteristics of aerosol size distributions and new particle
767 formation in the summer in Beijing, J. Geophys. Res. Atmos., 114(14), 1–13,
768 doi:10.1029/2008JD010894, 2009.
769 Zhang, Y. M., Zhang, X. Y., Sun, J. Y., Lin, W. L., Gong, S. L., Shen, X. J. and Yang, S.:
770 Characterization of new particle and secondary aerosol formation during summertime in
771 Beijing, China, Tellus, Ser. B Chem. Phys. Meteorol., 63(3), 382–394, doi:10.1111/j.1600-

0889.2011.00533.x, 2011.

Zheng, J., Khalizov, A., Wang, L. and Zhang, R.: Atmospheric pressure-ion drift chemical ionization mass spectrometry for detection of trace gas species, Anal. Chem., 82(17), 7302–7308, doi:10.1021/ac101253n, 2010.

Zheng, J., Hu, M., Zhang, R., Yue, D., Wang, Z., Guo, S., Li, X., Bohn, B., Shao, M., He, L., Huang, X., Wiedensohler, A. and Zhu, T.: Measurements of gaseous H_2SO_4 by AP-ID-CIMS during CAREBeijing 2008 Campaign, Atmos. Chem. Phys., 11(15), 7755–7765, doi:10.5194/acp-11-7755-2011, 2011.

Zheng, J., Yang, D., Ma, Y., Chen, M., Cheng, J., Li, S. and Wang, M.: Development of a new corona discharge based ion source for high resolution time-of-flight chemical ionization mass spectrometer to measure gaseous H_2SO_4 and aerosol sulfate, Atmos. Environ., 119, 167–173, doi:10.1016/j.atmosenv.2015.08.028, 2015.

Table 1 Mean, median, 5-95 % percentiles of key atmospheric variables and $[H_2SO_4]$ in the daytime.

	UVB ($W\ m^{-2}$)	$[SO_2]$ (ppbv)	CS (s^{-1})	$[O_3]$ (ppbv)	[HONO] (ppbv)	$[NO_x]$ (ppbv)	$[H_2SO_4]$ ($\times 10^6$ molecule cm^{-3})	RH (%)
mean	0.17	4.6	0.11	10.5	0.74	25.3	5.4	28
median	0.14	3.7	0.11	9.0	0.51	23.0	4.9	26
5-95% percentiles	0.00-0.45	0.9-11.4	0.01-0.24	3.5-23.3	0.09-2.65	3.3-61.4	2.2-10.0	9-59

Table 2 Correlation coefficients (Spearman type) between [H_2SO_4] and atmospheric variables in the daytime.

	UVB	[SO_2]	CS	[O_3]	[HONO]	[NO_2]	[H_2SO_4]
UVB	1	0.01	-0.02	0.14	-0.23	-0.04	0.46
[SO_2]		1	0.83	0.25	0.64	0.70	0.74
CS			1	0.36	0.75	0.77	0.60
[O_3]				1	-0.02	-0.04	0.29
[HONO]					1	0.88	0.39
[NO_2]						1	0.53
[H_2SO_4]							1

Table 3 Proxy functions for the nonlinear fitting procedure.

Proxy	Function[#]
N1	$k_0 \cdot UVB^a \cdot [SO_2]^b \cdot CS^c$
N2	$k_0 \cdot UVB^a \cdot [SO_2]^b$
N3	$k_0 \cdot UVB^a \cdot [SO_2]^b \cdot CS^c \cdot [O_3]^d$
N4	$k_0 \cdot UVB^a \cdot [SO_2]^b \cdot [O_3]^d$
N5	$k_0 \cdot UVB^a \cdot [SO_2]^b \cdot CS^c \cdot ([O_3]^d + [HONO]^e)$
N6	$k_0 \cdot UVB^a \cdot [SO_2]^b \cdot ([O_3]^d + [HONO]^e)$
N7	$k_0 \cdot UVB^a \cdot [SO_2]^b \cdot CS^c \cdot ([O_3]^d + [NO_x]^f)$

[#]UVB is the intensity of ultraviolet radiation b in W cm^{-3}; $[SO_2]$ is the concentration of sulfur dioxide in molecule cm^{-3}; CS is the condensation sink in s^{-1}; $[O_3]$ is the concentration of ozone in molecule cm^{-3}; [HONO] is the concentration of nitrous acid in molecule cm^{-3}; $[NO_x]$ is the concentration of nitrogen dioxide in molecule cm^{-3}; k_0 is a scaling factor.

Table 4 Results of the nonlinear fitting procedure for different proxy functions, together with correlation coefficient (R, Pearson type) and relative error (RE).

Proxy	k_0	a	b	c	d	e	f	R	RE (%)
N1	515.74	0.14	0.38	0.03				0.83	20.04
N2	280.05	0.14	0.40					0.83	20.00
N3	9.95	0.13	0.39	-0.01	0.14			0.85	19.95
N4	14.38	0.13	0.38		0.14			0.85	19.95
N5	0.0072	0.15	0.41	-0.17	0.36	0.38		0.86	19.11
N6	2.38	0.14	0.33		0.24	0.24		0.85	19.66
N7	0.0013	0.13	0.40	-0.17	0.44		0.41	0.86	19.34

Figure Captions

Figure 1. Correlations (a) between [H_2SO_4] and UVB intensity, and (b) between [H_2SO_4] and [SO_2] during the campaign from 9 February to 14 March, 2018.. k_m is a constant term.

Figure 2. Correlation between [HONO] and [NO_x] during the campaign from 9 February to 14 March, 2018. The black line represents a linear fitting with a zero intercept.

Figure 3. Performance assessments of proxy N2 and proxy N7. The REs are used to evaluate the performances of proxy N2 and N7, respectively as a function of linear bins of measured sulfuric acid concentrations.

Figure 4. Comparison of measured [H_2SO_4], $[H_2SO_4]_{N2}$, $[H_2SO_4]_{N7}$ and $[H_2SO_4]_{\text{Petäjä } et\ al.}$ on 10 March, 2018 with a time resolution of 5 min.

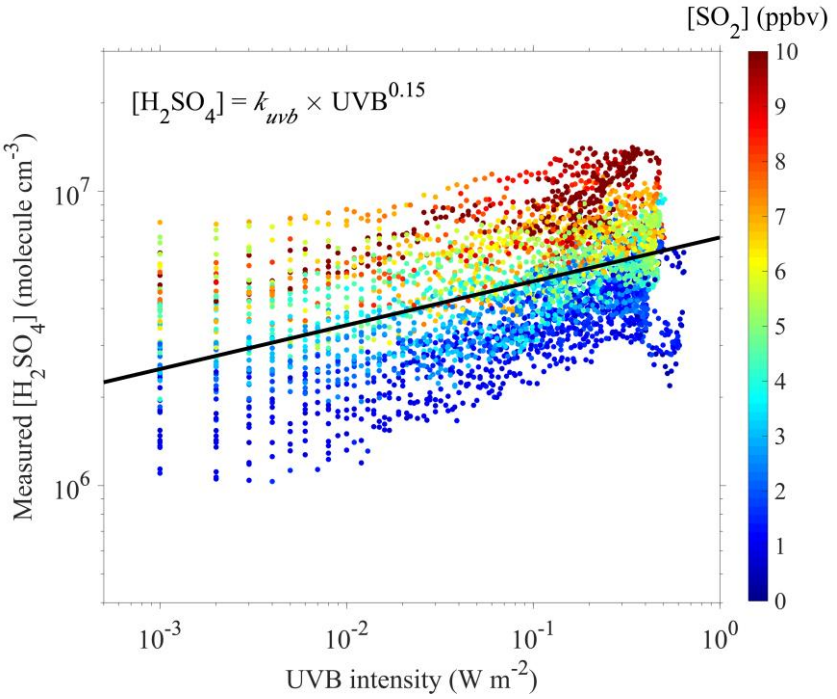

Figure 1a

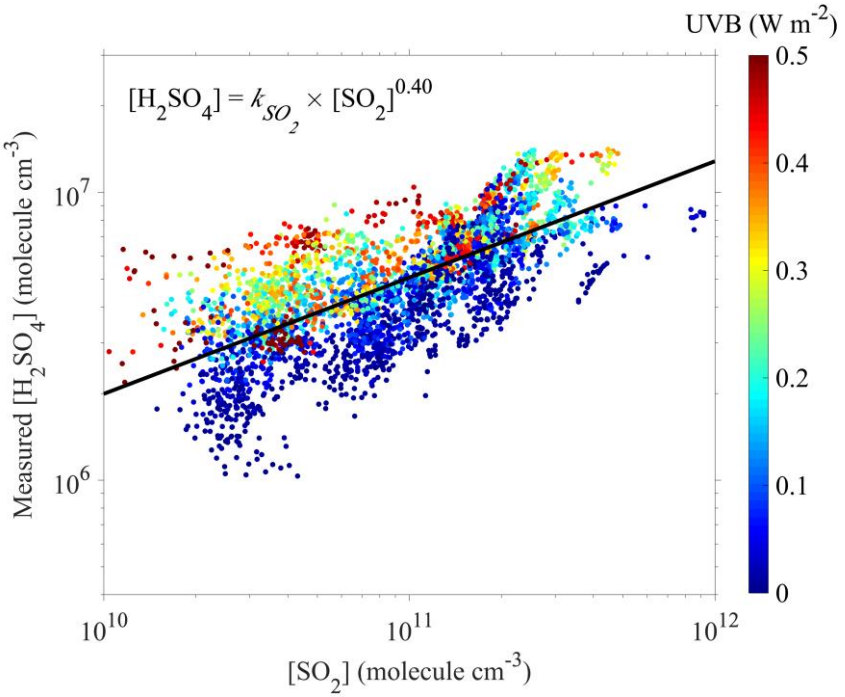

Figure 1b

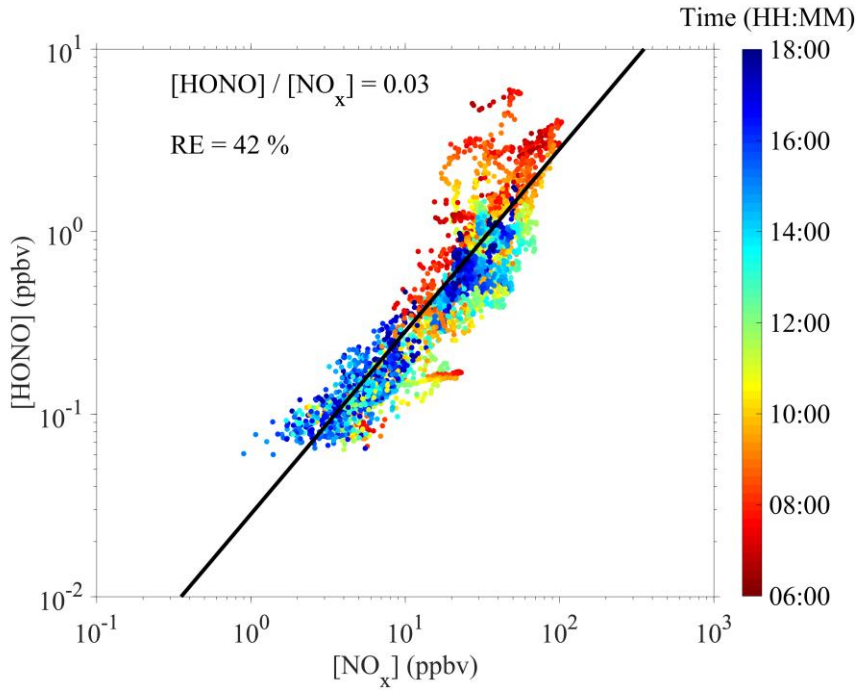
Time (HH:MM)
18:00
16:00
14:00
12:00
10:00
08:00
06:00
[HONO] / [NOx] = 0.03
RE = 42 %
[HONO] (ppbv)
[NOx] (ppbv)
10^1
10^0
10^-1
10^-2
10^-1
10^0
10^1
10^2
10^3

Figure 2

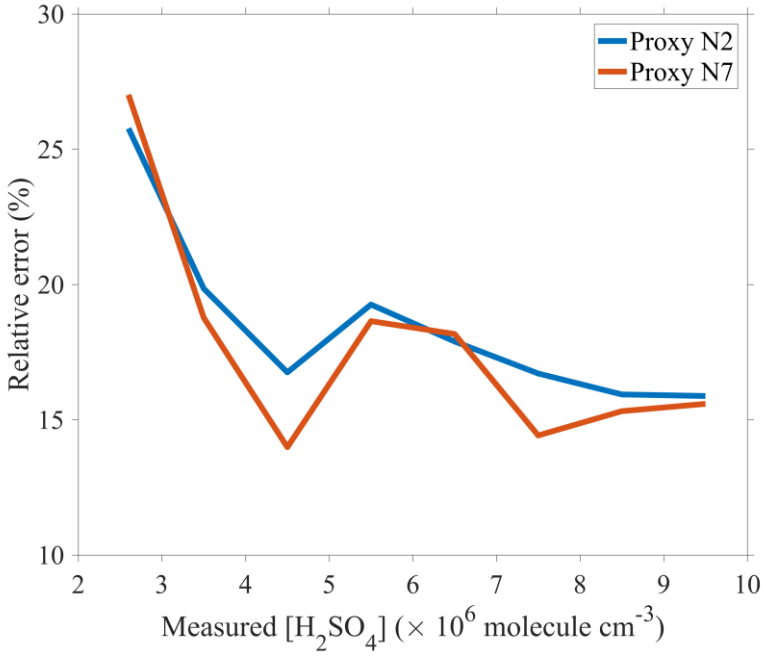
Proxy N2
Proxy N7
Relative error (%)
30
25
20
15
10
2
3
4
5
6
7
8
9
10
Measured [H2SO4] (× 10^6 molecule cm^-3)

Figure 3

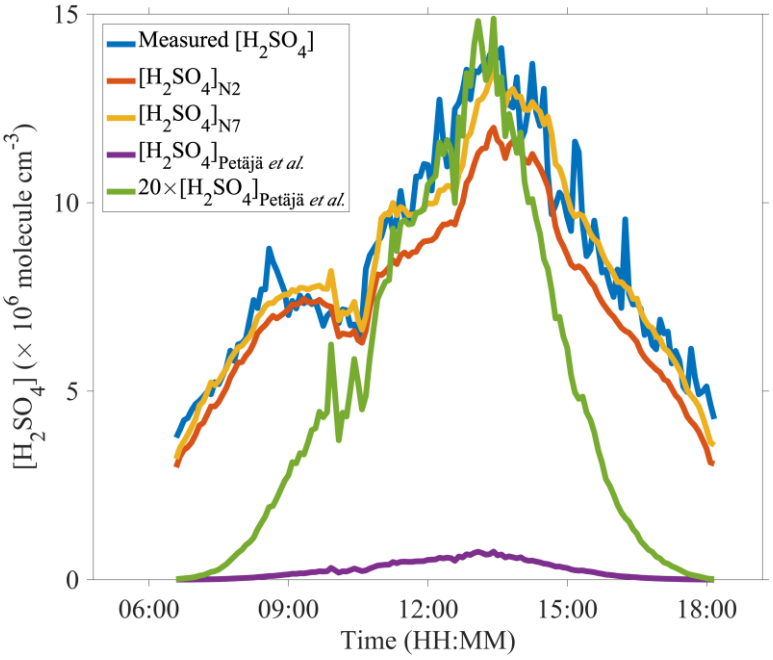
Measured [H2SO4]
[H2SO4]N2
[H2SO4]N7
[H2SO4]Petäjä et al.
20×[H2SO4]Petäjä et al.
[H2SO4] (× 10^6 molecule cm^-3)
15
10
5
0
06:00
09:00
12:00
15:00
18:00
Time (HH:MM)

Figure 4